Super-structured Fiber Bragg Gratings with improved features for Coherent Direct Sequence OCDMA

Rocío Baños[1], Daniel Pastor[1], Victor Garcia-Munoz[2] and Waldimar Amaya[1]

[1] *Instituto de Telecomunicaciones y Aplicaciones Multimedia*
Universitat Politècnica de València
8G Building - access D
Camino de Vera s/n - 46022 Valencia (Spain).

[2] *Phoenix Photonics Ltd. Sarre, CT7-0JZ ,(UK).*

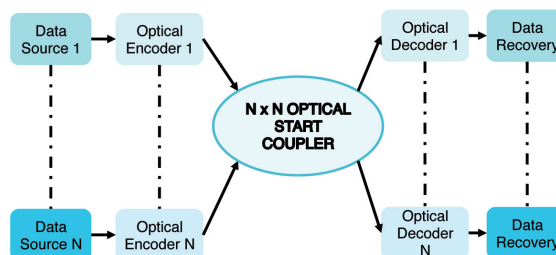*Corresponding author: dpastor@dcom.upv.es*

Abstract

This paper reports different proposals in the field of the Super-structured Fiber Bragg Gratings for Coherent Direct Sequence OCDMA applications providing enhanced features in terms of available spectral bandwidth, spectral efficiency and inter-channel rejection suitable for WDM and OCDMA combined applications. The reported devices cover the multiband en-decoders covering different bands on the same device, the almost rectangular envelope en-decoders demonstrated for both 1 and 5 ITU-100GHz bands providing flat response and a roll-off better than 5 dB/GHz, and finally a multidimensional WDM/CODE/SPACE multiplexing proposal based on the concatenation of rectangular SSFBGs.

Keywords: Coherent Direct Sequence (CDS) Optical Code Division Multiple Access (OCDMA), Super-structured Fiber Bragg Gratings (SSFBG). Wavelength Division Multiplexing (WDM).

1.Introduction to CDS-OCDMA systems

Coherent Direct Sequence (CDS) Optical Code Division Multiple Access (OCDMA) is presented as a promising technique that has attracted increasing attention for the implementation of FTTH over passive optical networks (PON) [1-3] or employed for optical en/decoding of headers (or labels) in Photonic Label Switching (PLS) networks [4-5]. CDS-OCDMA techniques has been demonstrated employing either integrated technology on Silica encoders [5-7] or Super Structured Fibre Bragg Gratings (SSFBG) [4,5,8,9]. Although Code division multiplexing (CDM) could be some times considered as an approach

too complex compared with their competitors as WDM-PON, it must be assumed as complementary technic for the future high bit-rate symmetric FTTH networks. It can be exploited in combination with WDM signals or conveyed into WDM bands as has been previously proposed by several authors [8-9], reducing the traditionally ultra-high bandwidth requirements and therefore the cost of the final devices. Moreover OCDMA techniques provide advantage in security against eavesdroppers on the physical medium. One example of the recent achievements to alleviate the practical limitations in the cost-sensitive field of access networking is the integrated multi-channel encoder [7] that can encode or decode numerous optical CDM channels simultaneously, and is suitable to be placed at the remote distribution node sharing the cost by the whole network. In this sense this paper focus on the SSFBG designs with upgraded features to be more efficiently employed in PON-WDM networks. We will present the multi-band en/decoder on the same device concept and its refinement on the rectangular envelope multiband en/decoder leading to the demonstration of a single band rectangular en/decoding device. Finally the multi-band & multi-code device is also proposed and demonstrated with clear application on optical en/decoding of headers in PLS networks.

■ **Figure 1.** *OCDMA PON.*

In this section we present the basic concepts supporting the encoding and decoding processes and we define the main parameters that we will refer along the paper. These fundamental concepts are independent of the network application or technology employed. The simplest scheme of OCDMA-PON is shown in Fig. 1. The encoding process begins with a short optical pulse that we can assume as a data bit from the OCDMA network user or owning to the label information sequence in PLS applications. This pulse must be encoded into a sequence of N sub pulses named "chips" that will be transmitted and reconstructed or decoded at the receiver nodes. The impulse response for the CDS device used for code "p" can be expressed as:

$$h_p(t) = h_{chip} \otimes \sum_{k=0}^{N} a_{p,k} \, e^{j\varphi_{p,k}} \bullet \, \delta(t\text{-}kt_{ch}) \qquad (1)$$

where $h_{chip}(t)$ is the individual chip impulse response given by the technology or the fabrications limitations, $a_{p,k}$ and $\varphi_{p,k}$ are the amplitude and phase defined by the code word "p" at the position "k" and t_{ch} is the time separation between input pulses. The spectral response can be written as:

$$H_p(\omega) = H_{chip}(\omega) \sum_{k=0}^{N} a_{p,k} \, e^{j\varphi_{p,k}} \bullet \, e^{jk\omega t_{ch}} \qquad (2)$$

$H_{chip}(\omega)$ is the global spectral envelope and corresponds to the Fourier transform of $h_{chip}(t)$ the summation term in (2) imposes a spectral periodic function with a Frequency Repetition Period (FRP) defined by $1/t_{ch}$. To accomplish the encoding and decoding process, the decoder devices should implement the reverse and conjugated code on it (3).

$$h_{decod}(t) = \left\{ h_{cod}(\text{-}t) \right\}^{*} \qquad (3)$$

Thus, the global system response can be expressed as the convolution of the input signal $x(t)$ and the impulse response of the encoder $h_P^{Cod}(t)$ and the decoder $h_q^{Decod}(t)$:

$$y_{p,q}^{system}(t) = x(t) \otimes h_P^{Cod}(t) \otimes h_q^{Decod}(t) \qquad (4)$$

Moreover, for simplicity the equation (4) can be rewritten as:

$$y_{p,q}^{system}(t) = h_{pulses}(t) \otimes h_{p,q}^{Cod/Decod} \qquad (5)$$

Where the first term is defined as $h_{pulses}(t) = x(t) \otimes h_{chip,p}(t) \otimes h_{chip,q}(t)$, which is the part related with the input pulse shape $x(t)$ and those of the encoder and the decoder. The part corresponding to the coding is:

$$h_{p,q}^{Cod/Decod}(t) = h_p^{Ideal} \otimes h_q^{Ideal}$$

$$h_{p,q}^{Cod/Decod}(t) = \{ \sum_{k=0}^{N} a_{p,k} \, e^{j\varphi_{p,k}} \bullet \, \delta(t\text{-}kt_{ch}) \} \otimes \{ \sum_{l=0}^{N} a_{q,l} \, e^{j\varphi_{q,l}} \bullet \, \delta(t\text{-}lt_{ch}) \} \qquad (6)$$

where $a_{p,k}$ and $\varphi_{p,k}$ correspond to the code word "p" at the position "k" imposed by the encoder, whereas $a_{p,l}$ and $\varphi_{p,l}$ correspond to the code word "q" at the position "l" imposed by the decoder.

At the receiver end after the optical decoding the correct decoded signals (proceeding from correct encoder and decoder pairs) will exhibit a strong peak named Autocorrelation Peak (ACP) surrounded of a low level like-noise signal named "wings". Whereas, non-correct combinations will generate just only the low level like-noise signal named in this case the Cross Correlation (XC) signal. Finally, in order to properly discern ACP from XC signals, it is required an electronic or optical *time gating* with duration of T_g [10] (with typical value around t_{ch}) and the final electronic processing and detection.

As we demonstrated in [11], the spectral content of the encoded signal (compound signal h_{pulses}) must have a bandwidth at least the order of FRP in order to take advantage of the complete encoding potential according to the code length (N). Furthermore, if this signal overpasses the FRP range, the ACP/XC ratio saturates to its theoretical maximum, only obtaining an inefficient use of the spectrum. This concept will be explored along the paper where we describe different proposals for more efficient WDM-OCDMA multi-channel utilization.

## 2. SSFBG Fabrication Process and Optical Bandwidth

As we said before, the non-limited spectral response of the ideal component $h_{i,j}^{Cod/Decod}$, is reduced by the frequency response of the individual technological elements that accomplish the en/decoding process $h_{chip}(t)$ which are defined by the fabrication process. The most employed technology based on the phase mask technique consists in the use of SSFBG structures that provide a local and distributed reflectivity along the whole interchip separation (t_{ch}) [7-9]. In this case, the device global spectral envelope $H_{chip}(\omega)$ corresponds to a "sinc-like" function [12] whose main lobe FWHM bandwidth is approximately equal to 0.9·FRP having strong notches at ±FRP. Consequently, only the main lobe can be employed to encode the signals. In order to increase the SSFBG bandwidth, we have proposed in [11] an SSFBG in which only a narrow region of the fiber ($\sigma_{chip,z}$) is inscribed, giving rise to a device whose bandwidth is independent of the inter-chip separation (t_{ch}), as it is illustrated in Fig. 2.

An example is depicted in Fig 3, which is a simulation for a 16-chip code length and summarizes two representative cases for a device with t_{ch}=10 ps with *Continuous* chips and *Gaussian* chips with $\sigma_{chip,t}$=2 ps. Note that the variation pattern in Fig. 3 is determined by the summation term which contains the code information (2). Based
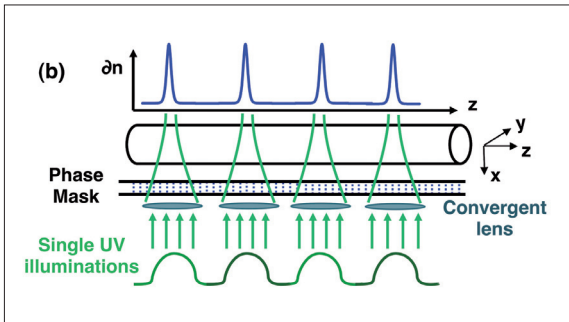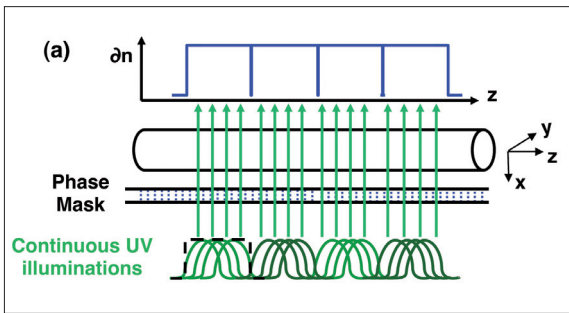
Figure 2. *(a) Continuous chip shape, (b) Short chips.*

on this behavior, broader FWHM bandwidth can be obtained if we are capable to minimizes the chip temporal width ($\sigma_{chip,t}$), which is defined by the ultraviolet laser beam width (σ_{UV}) employed ($\sigma_{chip,t} = (2 \cdot n/c) \cdot \sigma_{UV}$, where n is the fiber core refractive index and c the speed of light). We proposed the use of convergent lens placed between the UV laser and the phase mask to reduce the ultraviolet laser beam width as represented in Fig 2.
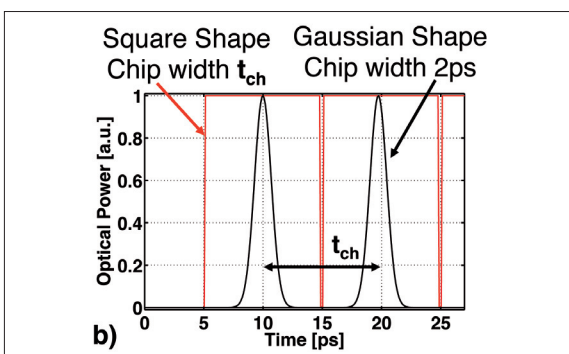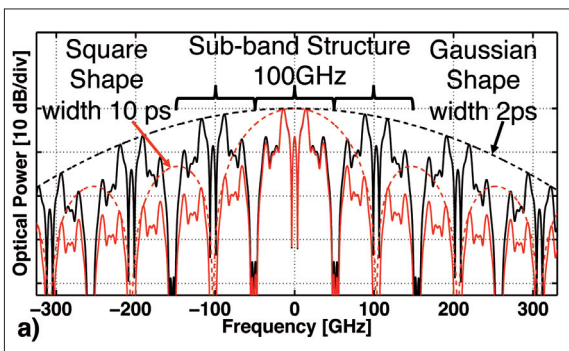

Figure 3. *(a) Multi-Band proposal by shortening the chip temporal width chip,t. (b) Chip temporal shapes.*

2.1.Multi-band en/decoding experimental verification

The multi-band (MB) en/decoding operation was verified employing the system setup shown in Fig. 4. Seven Multi-Band SSFBG en/decoders (two encoders and 5 decoders) were fabricated chip by chip with a focused Gaussian UV fringe pattern (~0,2 mm aprox.) and a chip separation fixed to 1 mm (t_{ch}=10ps).
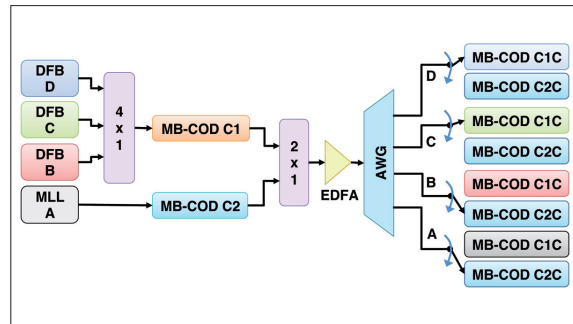

Figure 4. *System Setup.*

Figure 5 shows the spectral characterization of each fabricated devices for code 1. We can clearly identify the spectral repetition period of 100 GHz (0.8 nm) and the slow decaying envelope lower than 2 dB at 0.8 nm from maximum and 4 dB for 1.6 nm. Note that the obtained broadband spectral envelope can be employed for coding a single very broad band pulsed signal (like in a standard approach), or divided in sub-bands, as we propose here, in a WDM-OCDMA system employing narrower optical sources.
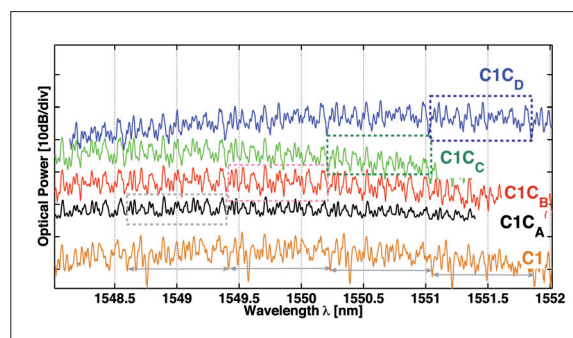

Figure 5. *Spectral response of the en/decoder devices implementing the code 1.*

To ensure a stable operation of the devices were placed into thermal boxes to compensate their detuning after fabrication. The seven MB-SSFBG devices are feed through the respective circulators. We employed four adjacent channels of an Array Waveguide Grating (AWG) router with 0.8 nm channel spacing and 0.4 nm 3dB bandwidth (channels A to D). The sources used were three DFB lasers pulsed by gain switching technique [13] at 1.25 Gpulses/s, and a

Mode Locked Laser (MLL) at 5 Gpulses/s rate before a Pulse Patter Generator (PPG) to reduce the pulse rate to 1.25 Gp/s. DFBs were combined by a splitter (4x1) and tuned to the three sub-bands (B to D), being codified in the same Multi-Band SSFBG C1 covering different portions of its spectrum. The MLL source was tuned from channels A to D and codified by Code 2. The en/decoding process was verified recovering the Auto-Correlation Peak (ACP) for the matched pairs (C1*C1c & C2*C2c) and the Cross-Correlation (XC) (C2*C1c & C1*C2c). See figures 6 and 7.
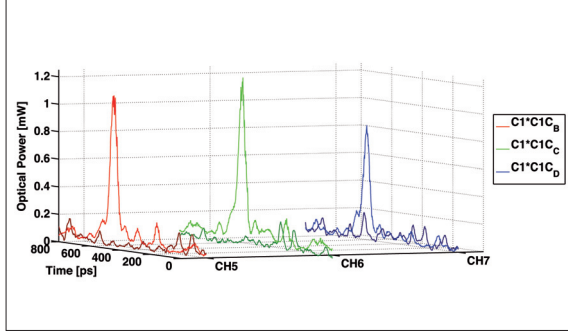
■ **Figure 6.** *ACP and XC signal for code 1.*
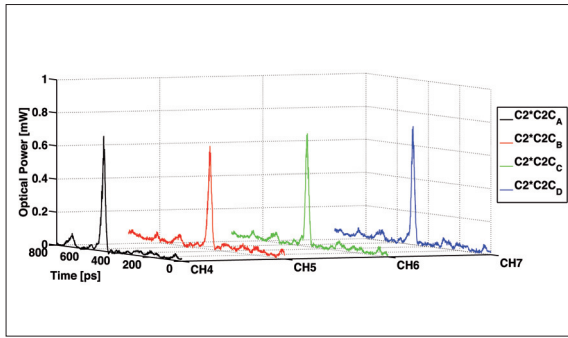
■ **Figure 7.** *ACP signal for code 2 using MLL source.*

ACP power was adjusted to the same value for all the cases to perform the ACP/XC ratio in the same interfering conditions and it was about 10 dB for the worst case.

3.Rectangular Envelope SSFBG En-Decoders

In the previous section Multi-Band SSFBG devices based on a Gaussian envelope were addressed, however, the slow decaying global envelope of the fabricated devices reduces the useable number of bands due to the power imbalanced among them. To solve this shortcoming, we have proposed [14] a more accurate design of the chip shape taking into account the influence of the fabrication process in order to reduce as much as possible its impact on the final device. The proposed solution compensates the Gaussian shape of the focalized UV beam to produce a new rectangular spectral envelope.

Taking up again the equation (2), we can rewrite it replacing H_{chip} by a Gaussian function $G(\omega)$:

$$H_p^{fabricated}(\omega) = G(\omega) \sum\nolimits_{k=0}^{N} a_{p,k}\, e^{j\,\varphi_{p,k}} \bullet e^{j\,k\omega t_{ch}} \quad (7)$$

Therefore, the system must be apodized with the inverse of the function $G(\omega)$, to mitigate the effect of the fabrication process. However, the inverse of $G(\omega)$ has very high values at frequencies separated from the central frequency due to it is a band pass signal. Consequently, the spectral response must be gated with a squared window function $W(\omega)$ [14]. Hence, the device to be fabricated should have the form described in (8), where the first term correspond to the ideal response, and the second term, $W(\omega)/G(\omega)$ named window apodization function ($H_{apod}(\omega)$).

$$H_p^{flat}(\omega) = \left[\sum\nolimits_{k=0}^{N} a_{p,k}\, e^{j\,\varphi_{p,k}} \bullet e^{j\,k\omega t_{ch}} \right] \bullet \left(\frac{W(\omega)}{G(\omega)} \right) \quad (8)$$

In the time domain $h_{apod}(t)$ is given by the convolution of the window with the inverse of the Gaussian function, where $w(t) = \mathfrak{S}^{-1}(W(\omega))$.

$$h_{apod}(t) = w(t) \otimes FT^{-1}\left[\frac{1}{G(\omega)} \right] \quad (9)$$

where $w(t) = FT^{-1}(W(\omega))$. This window apodization function with amplitude and phase imposes that the fiber is illuminated all along the complete chip during and ideally, if the focused UV beam corresponds with the employed $G(\omega)$, the device response after the fabrication can be written as [14]:

$$H_p^{reconstructed}(\omega) = H_{fabricada}(\omega) \bullet H_{apod}(\omega)$$

$$H_p^{reconstructed}(\omega) = H_{ideal}(\omega) \bullet G(\omega)) \bullet \left(\frac{W(\omega)}{G(\omega)} \right) \quad (10)$$

$$H_p^{reconstructed}(\omega) = \left[\sum\nolimits_{k=0}^{N} a_{p,k}\, e^{j\,\varphi_{p,k}} \bullet e^{j\,k\omega t_{ch}} \right] \bullet W(\omega)$$

obtaining the ideal response of the device only limited by the squared window function imposed. Figure 8a shows the schematic of the fabrication process where the h_{apod} function has a "sinc-like" shape for each individual chip. Figure 8b shows the rectangular envelope encoder for 5 bands equivalent to that shown in figure 2 without any compensation.
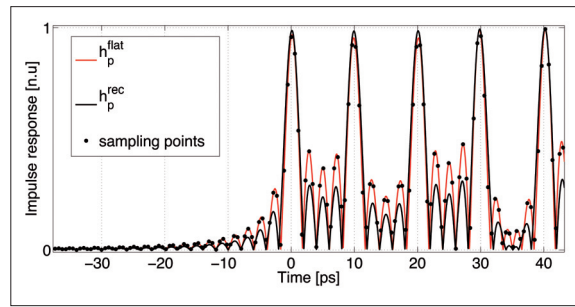
Additionally, in Fig 9 we can see the simulation results for the first five chips of the impulse response, the amplitude of the flat function $h_{p,}^{flat}$ the effective apodization obtained when the Gaussian sampling is performed h_p^{rec} and the sampling points to avoid overlapping in the central band and to perform a correct reconstruction.

These components open the feasibility to compact and spectrally efficient DWDM applications. In Figure 10 the different structures are compared in order to analyze their behavior in terms of crosstalk and spectral efficiency. The three spectral envelopes under consideration for an arbitrary 16 chips code are: a) Sinc-like envelope (rectangular chip shape caused by continuous illumination), b) Gaussian spectral envelope as designed before and c) Rectangular envelope (sinc-like shape for the chips). In all the

■ **Figure 9.** *Simulated impulse response of a 5 sub-band C1 encoder.*
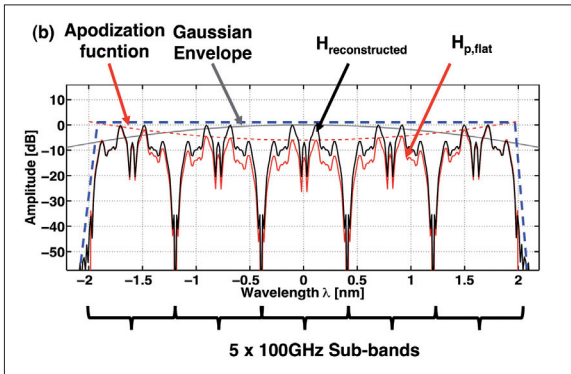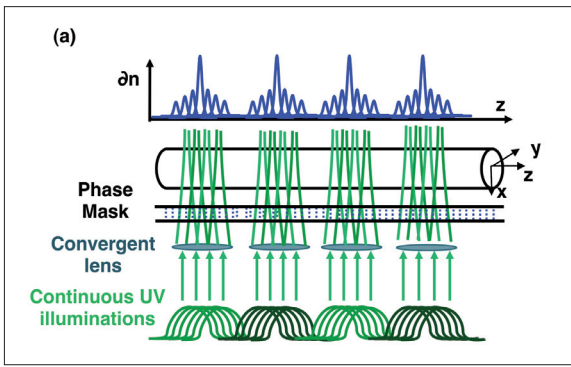
■ **Figure 8.** *Rectangular Envelope fabrication process (a) and results (b).*

cases t_{ch}=10 ps that correspond with a Frequency Repetition Period (FRP) of 100GHz. The maximum spectral efficiency will be bounded by the maximum inter-channel crosstalk and therefore by the spectral overlapping. The three different cases depicted in Fig. 10 show devices with different spectral separations and also with different number of available encoding bands. Notice that this is a generic WDM/multi-band OCDMA scenario where dif-

ferent devices could also have different codes. Figure 10(d) show the *averaged power crosstalk (xtalk)* for the most affected channels as a function of the optical frequency separation of the two WDM devices, and moreover the cases (a) to (c) corresponds with *-20dB of xtalk* illustrating the achievable *Spectral Efficiency defined as En-Decoding bandwidth / Total bandwidth* which are S= 1/3, ~2/3 and 1 respectively.

3.1. Experimental Results of Rectangular Envelope devices

Different devices were fabricated in order to show the practical feasibility of the proposed technique improving the performance in presence of crosstalk signals. In Fig 11, we can see the final devices fabricated using 5 and 1 sub-bands of 100GHz ITU Channels. The fabricated devices present less than 0.6 dB of total variation in reflectivity and a roll-off better than 5 dB/GHz. Experimental results using 5 and 1 sub-bands en/decoder combinations and their very good features of ACP/XC ratio demonstrate that these devices are suitable for both broadcasting and point-to-point applications, as we can see in Fig 12.
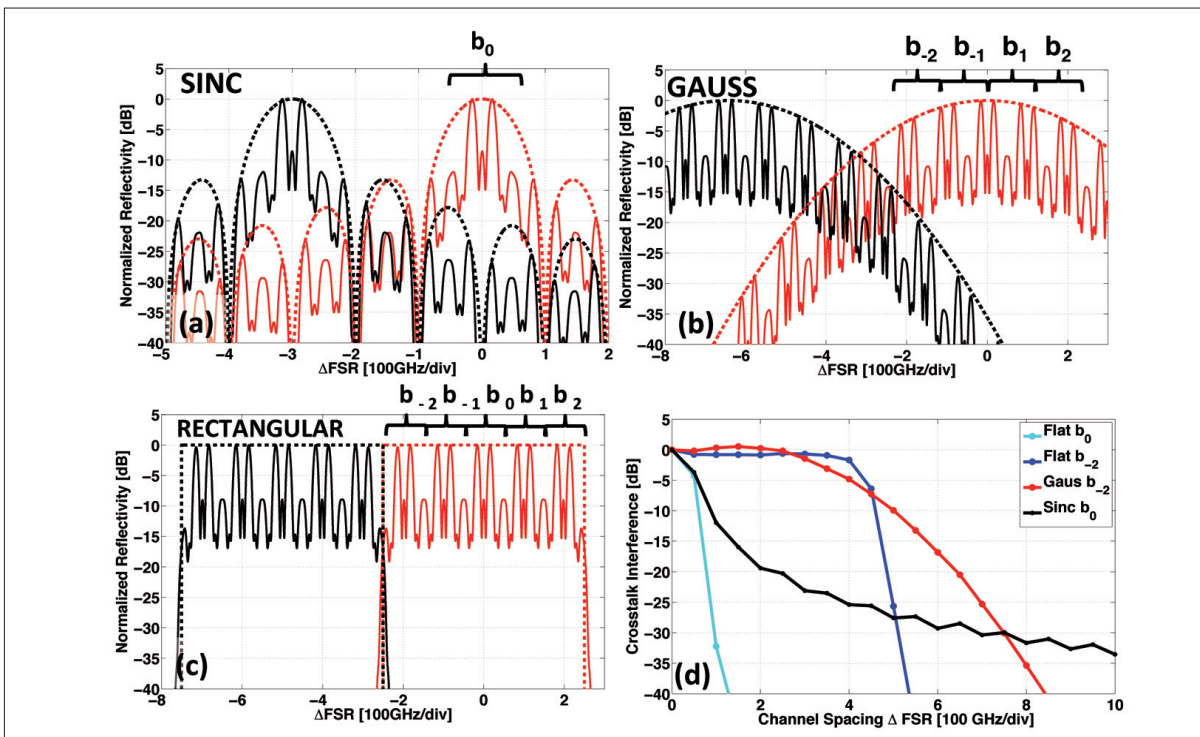
■ **Figure 10.** *Spectral efficiency and crosstalk.*

Fabricated devices provided almost rectangular enve-lope with uniformity better than 0.6 dB, roll-off at edges better than 5 dB/GHz and out of band rejection higher than 25 dB.
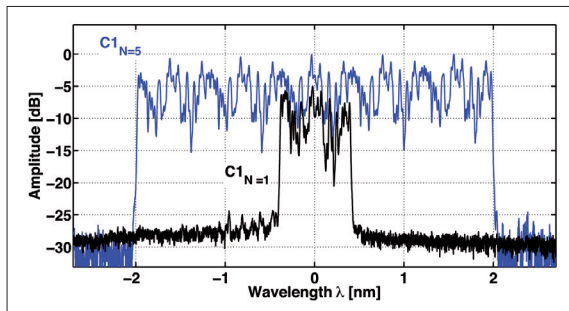
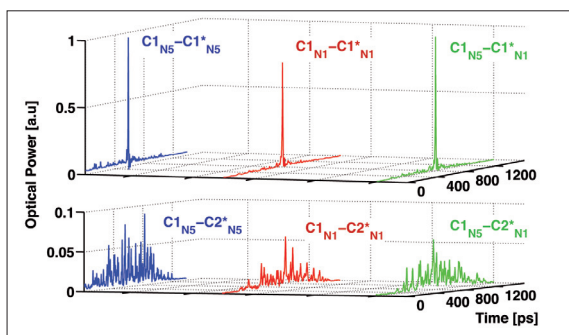■ **Figure 11.** *Fabricated device for 5 and 1 sub-bands.*

■ **Figure 12.** *ACP and XC signals.*

The rectangular envelope devices as demonstrated previously open the possibility of compact DWDM multi-band and multi-code devices. More specifically we have recently designed [15] a Dual-Code and Dual-Band device implementing two different codes in the same device. In Fig 13 a) we can see the final devices fabricated implementing different codes in order to accomplish the decoding process in a system where the encoding process is performed by a code-tunable Integrated En/Decoder (IED) device based on Silicon On Insulator. In this case the SSFBG and the IED implements an 8-length code, with a chip length of 1 mm (0.8 nm). The SSFBGs where de-

signed according to the inter-chip time $t_{ch}=10.5$ ps measured on the fabricated SOI devices. The selected spectral separation of the two different codes in each device was the double of the Frequency Repetition Period (FRP) $(1/t_{ch})$, i.e. $2(1/t_{ch})\approx190$GHz (~1.5 nm), in order to reserve a intermediate zone as guard-band to prevent interferences and the time separation was fixed to $2.5Nt_{ch}$ (~210 ps) in order to avoid overlapping of the ACP wings and XC signals. We fabricated 3 different device implementing 5 different code-words. The spectral response of the Dual Code SSFBGs fabricated and IED response are shown in Fig. 13 a), and the results obtained for the en/decoding process are shown in the Figure 13 b). In all the cases, the ACP/XC ratios obtained are in good agreement with the theory.

4. Conclusions

We have presented in this paper the recent achievements on Super-Structured Fiber Bragg Gratings designed for Coherent Direct Sequence OCDMA. The proper design and fabrication of the individual code element or "chip" inside the whole device represented a key aspect to construct the spectral envelope response giving rise to different proposals increasing the number of available channels and the spectral efficiency for the combined WDM-OCDMA systems. In the first proposal, the shortening of the chip duration led to broadband en-decoders with spectral envelopes embracing up to 5 encoding bands (FRP) on the same device. In order to increase the spectral efficiency for WDM approaches, it was proposed a complex chip profile to compensate the natural Gaussian envelope determined by the ultraviolet beam of the fabrication. In this case the designed and fabricated devices provided almost rectangular envelope presenting power uniformity better than 0.6 dB along of its five ITU-100GHz encoding channels and a roll-off better than 5 dB/GHz at the device edges with an out of band rejection higher than 25dB. Finally we describe the proposal of multi-band and multi-code devices based on multiple almost rectangular SSFBGs in chain. This structure integrates over a single device a multidimensional WDM/CODE/SPACE multiplexing.
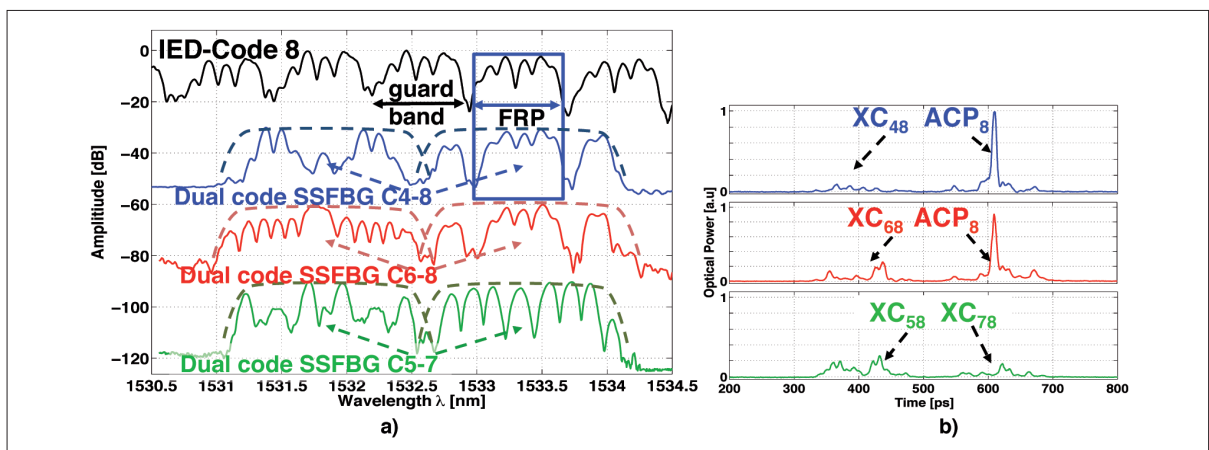

■ **Figure 13.** *Dual Code Rectangular Envelope SSFBG.*

Acknowledgments

References

[1] P. Green, "Paving the last mile with glass," IEEE Spectrum, vol. 39, no. 12, 13–14 (2002).

[2] L. H. Spiekman, "Active Devices in Passive Optical Networks", J. Lightwave Technology, vol. 31, no. 4, 488-495 (2013)

[3] K Kitayama, et al. "OCDMA over WDM PON-solution path to gigabit-symmetric FTTH," J. Lightwave Technology. 24, 1654-1662 (2006).

[4] X. Wang, et al. "Experimental demonstration of 511-chip 640 Gchip/s superstructured FBG for high performance optical code processing," in Proceedings of the Europeam Conference Optical Communication (ECOC), (Academic, Stockholm, Sweden, 2004), Paper Tu1.3.7.

[5] X. Wang and N. Wada, "Experimental Demonstration of OCDMA Traffic Over Optical Packet Switching Network With Hybrid PLC and SSFBG En/Decoders," J. Light. Technol., 24, 3012-3020, 2006.

[6] Xu Wang ; Naoya Wada ; T. Miyazaki ; G. Cincotti ; Ken-ichi Kitayama; Hybrid WDM/OCDMA for next generation access network. Proc. SPIE 6783, Optical Transmission, Switching, and Subsystems V, 678328 (November 26, 2007);

[7] N. Kataoka, N. Wada, G. Cincotti, and K.-I. Kitayama, "2.56 Tbps (40-Gbps 8-wavelength 4-OC 2-POL) asynchronous WDM-OCDMA-PON using a multi-port encoder/decoder," in Proc.ECOC, 2011, Postdeadline paper Th.13.B.6.

[8] P. C. Teh, et al., "Demonstration of a Four-Channel WDM/OCDMA System Using 255-Chip 320-Gchip/s Quaternary Phase Coding Gratings," IEEE Photon. Technol. Lett., 14, 227-229, 2002.

[9] H. Zheng et al; "Investigation of DWDM over OCDMA System Based on Parallelly Combined SSFBG Encoder/Decoders," in Proceedings of Symposium on Photonics and Optoelectronics (SOPO), (Academic, Wuhan, China, 2011), pp. 1-3.

[10] W. Amaya, et al. "Modeling of a Time-Spreading OCDMA System Including Nonperfect Time Gating, Optical Thresholding, and Fully Asynchronous Signal/Interference Overlapping," J. Light. Technol., 26, 768-776 (2008).

[11] W. Amaya, D. Pastor, R. Baños and V. Garcia-Munoz, "WDM-Coherent OCDMA over one single device based on short chip Super structured fiber Bragg gratings," Opt. Express, OSA, 19, 2011, pp. 24627-24637.

[12] M. Ibsen, M. Durkin, M. Cole, and R. Laming, "Sinc-sampled fiber Bragg gratings for identical multiple wavelength operation" Photonics Technology Letters, IEEE, vol. 10, n. 6, pp. 842 -844, June 1998.

[13] D. Pastor, et al. "Coherent Direct Sequence optical en/decoding employing low cost DFB lasers with narrow optical band consumption – towards realizable photonic label switching," in Proceedings of 12th International Conference on Transparent Optical Networks (ICTON), (Academic, Munich, Germany, 2010), pp. 1-4.

[14] Baños, R.; Garcia-Munoz, V.; Pastor, D.; Amaya, W., "Rectangular Global Envelope Super Structured FBGs for Multiband Coherent OCDMA," Photonics Technology Letters, IEEE , vol.25, no.5, pp.512,514, March1, 2013.

[15] Baños, R; Pastor, D.; Domenech, D.; " Code-Tunable Direct Sequence Coherent OCDMA device based on Silicon On Insulator," (Submitted to Transparent Optical Networks, 2013. ICTON '13).

Biographies

Rocío Baños, was born in Albacete, Spain, in 1986. She received the degree in Telecommunication Engineering from the Universidad Politécnica de Valencia, in 2010 and the MSc. degree in Telecommunication Technologies in 2012. In March of 2011 she joined the Optics and Quantum Communications Group at the Universidad Politécnica de Valencia. Currently, she is working on her research toward the Ph.D degree, which involves the design, fabrication and characterization of devices for optical code division multiple access (OCDMA) systems. Her research interests include Fiber Bragg Gratings for optical signal processing, optical networks and optical communications technologies.

Daniel Pastor, was born in Elda, Spain, on Novenber 5, 1969. He received the Ingeniero de Telecomunicacion degree in 1993, from the Universidad Politécnica de Valencia (UPV), and the Doctor Ingeniero de Telecomunicacion degree (Ph.D.) in 1996, from the Universidad Politécnica de Valencia, Spain. He joined the Departamento de Comunicaciones at the Universidad Politécnica de Valencia in 1993, where he was engaged to the Optical and Quantum Communications Group. From 1994 to 1998 he was a Lecturer at the Telecommunications Engineering Faculty and he became an Associate Professor since 1999. He is co-author of more than 120 papers in journals and international conferences in the fields of Optical Delay Line Filters, Fiber Bragg Gratings, Microwave Photonics, WDM and SCM ligthwave systems. He has been leader of national projects, related with Metro and Access optical Networks and Optical Code Division Multiple Access (OCDMA), and he has been leader of particular work packages in IST-LABELS (Ligthwave Architectures for the processing of Broadband Electronics Signals), or GLAMOROUS (Glass-based modulators, Routers and Switches). His current technical interests include Microwave Photonics, Complex Fiber Bragg Grating Fabrication for optical signal processing applications, WDM-SCM networks, RoF systems, and OCDMA techniques.

Victor Garcia-Muñoz received the M. Sc. in physics degree from the Universidad de Valencia, Spain and the Nuclear Physics Master Degree from the Université de Paris XI, France both in 2001. In 2002 he was at the Universita di Pavia working in the field of microwaves. He completed his Ph.D. in the Photonics Technology Group at the Universidad Politécnica de Madrid in 2008. His dissertation subject was related with the applications of Fiber Bragg Gratings (FBGs) to the processing of ultrafast optical signals. From June 2008 to August 2009 we worked at the Université Polytechnique de Mons, Belgium where he was involved in the study and reduction of the polarization related properties of FGBs and in the applications of in-fiber sensing techniques to the fabrication of composite pieces. In Aeptember 2009 he joined the Optics and Quantum Communications Group at the Universidad Politecnica de Valencia as a Juan de la Cierva fellow where he worked on the fields of Quantum Key Distribution and Optical Code Division Multiple Access (OCDMA). In May 2012 he joined Phoenix Photonics Ltd where he develops polarization related devices and passive optical devices for optical Space Division Multiplexing communications.

Waldimar Amaya, was born in Bogotá, Colombia. He received the Electronics Engineer, Mobile Telecommunications Specialist, and M.Sc. degrees from the Distrital University, Bogotá, Colombia, in 1999, 2000, and 2006, respectively. For two years, he was a Hybrid Fiber Coaxial Community Access Television Operator. Later, he was an Assistant Lecturer at two universities in Colombia. In 2005, he joined the Optical and Quantum Communications Group (OQCG), Institute of Telecommunications and Multimedia Research Institute - iTEAM, where he developed his PhD thesis and he obtained his PhD degree in telecommunications from the Universidad Politecnica de Valencia (UPV) Valencia, Spain, in 2008. Since 2009 he works with the OCQG – iTEAM as fellow research where he has continued with his work in optical signal processing and more recently in the field of quantum key distribution.